Fingertip positioning and tracking method of intelligent moving bracelet based on improved Kalman filter

Honggang Zheng

Physical Education and Research Department,
Changchun Institute of Architecture,
Changchun, Jilin, China
Email: honggang@mls.sinanet.com

Abstract: In order to overcome the problems of poor positioning accuracy and low tracking accuracy of traditional methods, this paper proposes an intelligent motion bracelet fingertip positioning and tracking method based on improved Kalman filter. Firstly, the bracelet signal filtering is realised by the least square method; the Z-score method is used to normalise the sensor pressure data to realise data pre-processing; then, the rigid structure model of human hand bone is constructed, the posture of human hand is reconstructed, the coordinate system of human upper arm is obtained, and the positioning ability of fingertip is improved. Finally, the RSSI signal of fingertip is collected by sensor, and the improved Kalman filter is used to realise the positioning and tracking of fingertip of bracelet. The experimental results show that the positioning accuracy of this method is 97.9%, the tracking accuracy is 97.6%, and the fingertip positioning and tracking effect is good.

Keywords: KNN algorithm; Z-score method; low pass filter; least square method.

Reference to this paper should be made as follows: Zheng, H. (2022) 'Fingertip positioning and tracking method of intelligent moving bracelet based on improved Kalman filter', *Int. J. Product Development*, Vol. 26, Nos. 1/2/3/4, pp.242–253.

Biographical notes: Honggang Zheng received his Master's degree in Curriculum and Education theory from Northeast Normal University in 2008. Now, he is awarded the title of Lecturer. In 2014, he worked in Changchun Institute of Architecture, Jilin Province, China, as the school's Physical Education Teacher and Head Coach of Volleyball Team.

1 Introduction

Intelligent wearable devices play a more and more important role in the scene of human-computer interaction. In particular, smart watches, bracelets and other devices can be naturally worn on the wrist by users. Human actions can be easily and effectively recognised and analysed through various built-in motion sensors, such as motion type recognition and micro gesture recognition (Xu et al., 2020; Ma et al., 2019; Yao et al., 2019). Among them, the movement type recognition function is closely related to people's daily activities. The bracelet can identify the user's current movement type and movement time, count and analyse the user's daily movement, then feed back to the user and provide appropriate exercise suggestions (Xu and Hu, 2019). Micro-gesture recognition plays an important role in smart home and other scenes. By wearing a bracelet to capture the micro gesture action of the human body, the user can control the smart device at home in real time. This interaction is very natural and convenient (Wu and Feng, 2019). At the same time, compared with the vision based scheme, it is easy to be limited by light and angle of view, and the scheme based on acoustic signal and wireless signal is easy to be affected by the surrounding environment. Intelligent wearable devices have the characteristics of portability, good concealment and long continuous working time. Therefore, relevant scholars have studied this and made some progress.

Liu and Gong (2019) proposed a fingertip positioning algorithm based on multi-objective distribution estimation, tracked the moving route of human fingertip position through ant colony algorithm, constructed the fingertip moving position change model, solved the fingertip position change model through distribution estimation algorithm, and used the minimum sampling variance to obtain the best value of fingertip positioning to realise fingertip positioning, The fingertip positioning speed of this method is fast, but the positioning accuracy is low. Chen et al. (2019) tracked the underwater robot target by introducing a deep learning method, simulate the robot to enhance the underwater target image through monocular vision technology, complete the target image feature extraction through deep learning and obtain the image depth information according to iterative training. This method can improve the robot target tracking effect, but the target accuracy of this method is poor. Chen (2020) introduced the image tracking method to locate and track the human moving target, used the edge contour detection to obtain the target position, obtained the three-dimensional surface information of the target image and determined the position of the human moving target through the corner detection method. This method can obtain a more accurate target position, but the position tracking accuracy needs to be improved.

To solve the above problems, this paper proposes an intelligent motion Bracelet fingertip positioning and tracking method based on Improved Kalman Filter. The specific research ideas are as follows:

Firstly, the signal of intelligent sports bracelet is filtered by least square method, and the high-frequency noise is filtered by low-pass filter; The *Z*-score method is used to normalise the pressure data of the sensor to realise the standardised processing of the motion Bracelet signal;

Secondly, according to the pre-processing results, the rigid structure model of human hand bone is established, the human hand posture is reconstructed, the human upper arm coordinate system is obtained, and the fingertip positioning ability is improved;

Then, the hidden Markov model is initialised, the observation probability matrix is calculated, and the maximum position of state transition probability is obtained; The state transition matrix is calculated by the improved Kalman Filter algorithm to obtain the grid with the largest state transition probability. At this time, the grid points are the fingertip positioning and tracking results of the intelligent moving bracelet;

Finally, the full text is summarised.

2 Data acquisition and pre-processing of sports bracelet

The original timing signal flow in the moving bracelet is expressed as $S = \{(x_1, y_1), (x_2, y_2), ..., (x_T, y_T)\}$, where x_1 represents a multi-dimensional vector corresponding to time t (where, $1 \le t \le T$), $y_t \in R^d$ represents the existence of different sensor channels, and T represents the total length of the time series (Zhang et al., 2021). Because the collected acceleration sensor signal often contains noise, denoising is needed to obtain relatively pure data (Duan et al., 2020). We use Savitzkygolay smoothing filter (which filters the signal in time domain according to polynomial least square method) to reduce the random noise of the signal. The specific operations are as follows: m convolution coefficients C_i are selected to process the three-axis timing data, respectively:

$$Y_t = \sum_{i=1-m/2}^{m-1/2} C_i y_{t+i} \quad \frac{m-1}{2} \le t \le T - \frac{m-1}{2} \tag{1}$$

$Y_t \in R^d$ is the value of the three-axis sensor corresponding to the time t after filtering. Compared with the traditional smoothing filter, the biggest feature of Savkzkygoky filter is that it can filter out the noise and ensure that the shape and width of the signal remain unchanged, so as to reduce the impact of smoothing on useful information as much as possible (Tian et al., 2019). It is generally believed that the frequency of human body during normal movement is low, but it is usually accompanied by high-frequency body jitter. This part of high-frequency signal is often noise data, and high-frequency noise can be filtered out by introducing a low-pass filter (Liu et al., 2020). Since the collected sensor data unit is 1/256 gravitational acceleration (*g*), it is necessary to divide the data by 256 and multiply it by the standard gravitational acceleration (9.80) (m/S^2) as the unit data. When different users perform the same motion, there are usually problems of different strength and amplitude, resulting in inaccurate motion type recognition. Therefore, we use the *Z*-score method to normalise the data and convert the triaxial acceleration data into a data stream with mean value of 0 and standard deviation of 1 (Zhang and Hu, 2020).

Using the *Z*-score normalisation processing method, it is advisable to set the time series data of a sitting posture as $a_1, a_2, ..., a_n$, then:

$$a_i^* = \frac{a_i - \bar{a}}{\sigma} \tag{2}$$

where $\bar{a}$ is the mean value of $a_1, a_2, ..., a_n$ and σ is the standard deviation. $a_1^*, a_2^*, ..., a_n^*$ is dimensionless data, their mean is 0 and their variance is 1.

According to the normalised results, the fingertip positioning and tracking of intelligent motion bracelet is carried out.

3 Fingertip positioning and tracking method of intelligent moving bracelet based on improved Kalman filter

3.1 Posture reconstruction of human hand and acquisition of upper arm coordinate system

In the fingertip positioning of intelligent sports bracelet, compared with the lower limbs, the upper limbs participate in more activities and have a wider range of activities. Taking the human upper limb as an example, according to the approximate human anatomy theory (Xiu et al., 2019), the human upper limb is defined as a 9-segment bone rigid body structure model, as shown in Figure 1.

Figure 1 Human skeleton model modelling

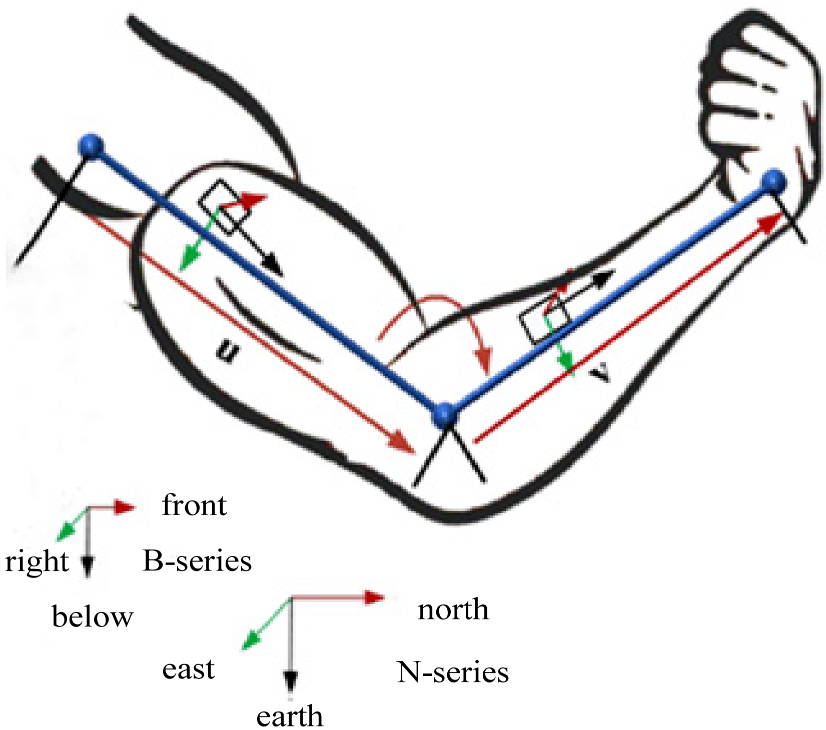

Shoulder, elbow and waist joints can move freely and other bone segments are rigidly connected. The length of each bone can be manually defined according to the actual situation of athletes. Special clothing is used to wear six data acquisition nodes on the waist (node1), trunk (node2), left upper arm (node3), left forearm (node4), right upper arm (node5) and right forearm On (node6), each data acquisition node can be regarded as rigidly connected with the corresponding bone segment. Node2 is responsible for measuring the motion data of head, left shoulder, right shoulder and trunk and the other nodes measure the motion data of their attached bone segments respectively. Each bone segment of the human hand in the model can be represented by a vector, that is, the bone segment vector at any time in the B system can be defined as $v_b = \left[v_x, v_y, v_z\right]$ and expressed as $v_b = \left[0, v_x, v_y, v_z\right]$ in the form of quaternion. Initially, the human body stands upright and shrinks to the O_yz plane of the human body coordinate system. At this time, the unit vector $v_{b,unit}$ of each bone segment in the B system and the vector of each joint segment of the athlete can be calculated by equation (3):

$$v_b = l \cdot v_{b,unit} \tag{3}$$

where l is the actual length of the athlete's bone segment. Theoretically, at any time, the vector v_b in the v_b system can be rotated to the N system through the attitude quaternion, $q_{b,t}^n$ as shown in equation (4).

$$v_{n,t} = q_{b,t}^n \otimes v_b \otimes \left(q_{b,t}^n\right)^* \tag{4}$$

$q_{b,t}^n$ represents the rotation quaternion from *B* system to N system at time *t*, which can be calculated by the following formula.

$$q_{b,t}^n = q_{s,t}^n \otimes q_{b,t}^s \tag{5}$$

where $q_{b,t}^s$ represents the rotation relationship between *B* system and *S* system at time *t*.

According to the establishment principle of human bone model, it is considered that the data acquisition nodes are closely connected with their corresponding bone segments (Chen and Li, 2020). Therefore, we assume that the rotation relationship between *B* system and *S* system is constant, and the rotation relationship at any time is replaced by the rotation relationship at the initial time, that is, $q_{b,t}^s = q_{b,init}^s$. At the initial moment, the athlete needs to face the north, keep his body vertical, stand still for 3 to 5 seconds, and complete the initial posture solution. At this time, the athlete's upper arm coordinate system (*B* system) coincides with the navigation coordinate system (*N* system), so there is the following relationship:

$$q_{b,init}^s \approx q_{n,init}^s \tag{6}$$

$$q_{n,init}^s = \left(q_{n,init}^s\right)^* \tag{7}$$

Thus, $q_{b,t}^s$ can be calculated from equation (15)

$$q_{b,t}^n = q_{s,t}^n \otimes \left(q_{s,init}^n\right)^* \tag{8}$$

According to the constructed athlete's upper arm coordinate system, the next intelligent movement Bracelet fingertip positioning and tracking is carried out.

3.2 Fingertip positioning and tracking of intelligent motion bracelet based on Improved Kalman Filter

In order to realise the fingertip tracking and positioning of intelligent moving bracelet, the RSSI signal is collected by the sensor, the fingertip positioning results of KNN algorithm are used and the fingertip positioning and tracking design steps of intelligent moving Bracelet by improving Kalman Filter algorithm are as follows:

1) *Calculate the initial value of KNN positioning:* Firstly, the hidden Markov model can be defined as $\lambda = \{\pi, A, B\}$, The real-time RSSI signal is compared with the information in the database by KNN algorithm to obtain the positioning results. In this subject, HMM algorithm uses Euclidean distance as the standard for similarity measurement between online RSSI samples and offline RSSI samples (Zheng et al., 2020).

2) *Initialise hidden Markov model*:

$$\delta_i = \pi_i r_i(o_1) \tag{9}$$

Create vector δ and initialise. Determine the KNN initial position state probability distribution π, π_i represents the probability that the measurement point appears at a certain position in the grid at the initial time. This topic assumes that π follows a uniform probability distribution, that is, the probability of initial position distribution is equal. Set the state transition matrix A, $A = \{a_{ij} = P(S_j = j \mid S_i = i)\}(1 \le i, j \le N)$, a_{ij} is the probability of transferring from position i to position j. In this subject, set the probability of two-dimensional plane vertex to adjacent point as 1/3, and the probability of plane edge to adjacent point as 1/4. Only when position i and position j are adjacent, the transition probability is not zero, and it can be obtained:

$$\sum_{\mathrm{j=1}}^{\mathrm{N}} a_{ij} = 1 0 \le a_{ij} \le 1 \tag{10}$$

3) *Calculation of observation probability matrix*:

$$r_i(k) = \begin{cases} \dfrac{1}{|p_i - p_k|} & (|p_i - p_k| \ne 0) \\ 1 & |p_i - p_k| = 0 \end{cases} \tag{11}$$

R is the observation probability matrix, and $R = \{r_i(k) = P(O_i \mid S_{i-1})\}$, $r_i(k)$ is the observation probability when the observation state is O_i at time i. This subject $r_i(k)$ takes the reciprocal distance between the initial position obtained by KNN algorithm and each grid point as the observation probability.

4) *Get the position with the maximum state transition probability*:

$$\begin{cases} \delta_t(j) = \max\limits_{1 \le i \le N} \left[\delta_{t-1}(i) a_{ij}\right] r_i(o_t) \\ \psi_t(j) = \operatorname*{argmax}\limits_{1 \le i \le N} \left[\delta_{t-1}(i) a_{ij}\right] \end{cases} 2 \le t \le T, 1 \le j \le N \tag{12}$$

Traverse all possible transition states of the current state and check the abnormalities (including abnormal human action behaviours such as running, falling, retrograde, wandering, etc.) to calculate the transition state with the highest probability, and N is the sum of the number of reference points. If the observation probability of a grid is multiple times higher than that of the current grid itself and adjacent grids (the positioning and tracking algorithm in this paper selects 15 times according to multiple tests), an exception will be handled.

The initial value of the hidden Markov model is obtained by the Bluetooth fingerprint location algorithm. Here, the *k*-nearest neighbour algorithm is used. The initial value of the fingerprint location is used as the observation value of the hidden Markov model to calculate the state transition probability. After calculating the state transition matrix, find out the grid with the largest state transition probability. At this time, the grid points are the positioning and tracking results of the fingertips of the intelligent mobile bracelet

4 Experiment

4.1 Experimental scheme

The subjects of this study were three sports bracelets (Xiaomi Bracelet 4, Huawei Bracelet 4 and Fitbit versa 2, 2 for each). The subjects were 20 healthy male college students from the school of physical education and training of Shanghai Institute of physical education (age 23.8 ± 1.8 yrs, height 176.4 ± 5.6 CM, weight 74.0 ± 9.4 kg). The basic information of the subjects is shown in Table 1. All participants were provided with written instructions outlining the research procedures, but were not informed of the purpose of the study.

Table 1 Basic characteristics of subjects

Number	*Age*	*Height/cm*	*Weight/kg*	*Body fat ratio/%*	*Training years/ yrs*
001	21	182	70	15	2
002	20	186	88.4	25	3
003	25	178	72	20	8
004	21	179	66	16	7
005	22	176	71	20	3
006	23	189	71	12	8
007	25	192	76	15	7
008	26	173	70	19	5
009	24	178	76	17	8
010	22	179	71	18	6
011	29	169	70	20	12
012	24	170	70	16	5
013	24	185	68	19	8
014	24	181	78	21	5
015	23	172	68	19	3
016	22	175	64	18	2
017	20	168	65	23	5
018	23	179	99.5	28	6
019	25	172	63	20	8
020	26	179	70	17	3
Average Value	23.45	178.1	72.345	18.9	5.7
Standard Deviation	1.8	5.6	9.4	8.2	3.8

This study is a random equilibrium crossover design. All subjects need to participate in 8 tests in the indoor field. Within one week before the formal test, all subjects came to the site to familiarise themselves with the equipment and test process, And learn the subjective perception scale At the end of the familiarity phase, ensure that all subjects understand and adapt to the test. At the same time, inform the subjects of the relevant requirements during the test, that is, all subjects should ensure adequate sleep during the test, maintain normal eating habits, avoid high-intensity training or exercise and alcohol intake 24 hours before the test, and avoid caffeine drinks or food intake 6 hours before the test. Each test before starting, the subjects shall truthfully fill in the compliance with various requirements to confirm that they meet the specified requirements of the experimental test. Then, the subjects were warmed up for 10min (5min jogging + 3min specific speed angle change running) (be familiar with the corresponding speed angle change running + 2min dynamic stretching in the current test). After warm-up, sit still for 5min. During this period, the tester will wear the heart rate band and 6 sports bracelets of Xiaomi, Huawei and Fitbit. After wearing the heart rate band and sports bracelet, the subjects will randomly participate in any speed under any direction change angle (90° and 180°) (4, 6, 8, 10km/h) direction change run test, the test duration is 5 min. In order to reduce the interaction between tests, the time between two tests is > 24 h.

4.2 Experimental index

Because motion recognition is a common classification problem, in the experiment, we use the following evaluation indexes to measure the performance of the algorithm model, namely accuracy and accuracy

1) *Accuracy rate*: The accuracy rate P_{re} represents the proportion of correctly predicted samples among the samples predicted as positive examples, and its calculation formula is:

$$P_{re} = \frac{T_p}{T_p + F_p} \tag{13}$$

In the formula, T_p represents the number of positive samples correctly predicted as positive by the model, and F_p represents the number of negative samples incorrectly predicted as positive by the model

2) *Precision*: Accuracy A_{cc} represents the proportion of correctly predicted samples in all samples, and its calculation formula is:

$$A_{cc} = \frac{T_p + T_n}{T_p + F_n + F_p + T_n} \tag{14}$$

In the formula, F_n represents the number of positive class samples incorrectly predicted as negative class by the model, and T_n represents the number of negative class samples correctly predicted as negative class by the model.

4.3 Experimental results

In order to verify the positioning and tracking effect of this method on the fingertip of intelligent moving bracelet, the methods in Liu and Gong (2019), Chen et al. (2019) and this method are used to count the positioning and tracking accuracy. The results are shown in Figure 2.

Figure 2 Finger tip positioning and tracking accuracy of intelligent motion bracelet

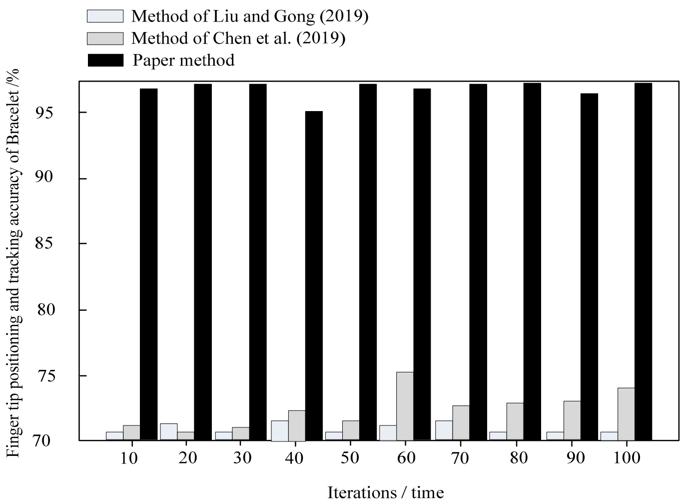

It can be seen from the analysis of Figure 2 that when the number of iterations is 30, the fingertip positioning and tracking accuracy of the intelligent moving Bracelet method in Liu and Gong (2019) is 70.5%, the fingertip positioning and tracking accuracy of the intelligent moving Bracelet method in Chen et al. (2019) is 72% and the fingertip positioning and tracking accuracy of the intelligent moving Bracelet method in this paper is 97.3%. When the number of iterations is 80, the fingertip positioning and tracking accuracy of the intelligent moving Bracelet method in Liu and Gong (2019) is 71%, the fingertip positioning and tracking accuracy of the intelligent moving Bracelet method in Chen et al. (2019) is 73.5% and the fingertip positioning and tracking accuracy of the intelligent moving Bracelet method in this paper is 98%. When the number of iterations is 100, the fingertip positioning and tracking accuracy of the intelligent moving Bracelet method in Liu and Gong (2019) is 71%, the fingertip positioning and tracking accuracy of the intelligent moving Bracelet method in Chen et al. (2019) is 74%, and the fingertip positioning and tracking accuracy of the intelligent moving Bracelet method in this paper is 97.8%. The method in this paper always has a high positioning and tracking accuracy of the fingertip of the bracelet, which shows that the method in this paper has a good tracking accuracy.

In order to verify the positioning and tracking effect of this method on the fingertip of intelligent moving bracelet, the methods Liu and Gong (2019), Chen et al. (2019) and this method are used to verify the accuracy of positioning and tracking. The results are shown in Figure 3.

Figure 3 Fingertip positioning and tracking accuracy of intelligent motion bracelet

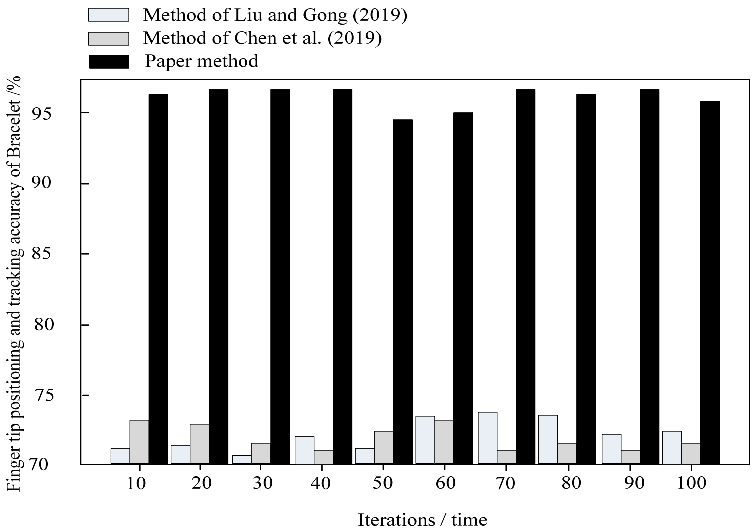

According to the analysis of Figure 3, when the number of iterations is 10, the positioning and tracking accuracy of the moving Bracelet fingertip of the method in Liu and Gong (2019) is 71.5%, the positioning and tracking accuracy of the moving Bracelet fingertip of the method in Chen et al. (2019) is 73% and the positioning and tracking accuracy of the moving Bracelet fingertip of the method in this paper is 97%. When the number of iterations is 50, the positioning and tracking accuracy of the moving Bracelet fingertip of the method Liu and Gong (2019) is 71.5%, the positioning and tracking accuracy of the moving Bracelet fingertip of the method in Chen et al. (2019) is 72.5% and the positioning and tracking accuracy of the moving Bracelet fingertip of the method in this paper is 94%. When the number of iterations is 100, the positioning and tracking accuracy of the moving Bracelet fingertip of the method in Liu and Gong (2019) is 72.5%, the positioning and tracking accuracy of the moving Bracelet fingertip of the method Chen et al. (2019) is 71% and the positioning and tracking accuracy of the moving Bracelet fingertip of the method in this paper is 95.2%. The accuracy of fingertip positioning and tracking of moving Bracelet in this method is higher than that of other methods, which shows that this method can improve the effect of fingertip positioning and tracking of bracelet.

5 Conclusions

This paper presents a fingertip positioning and tracking method of intelligent moving Bracelet based on Improved Kalman Filter. Firstly, the signal of the intelligent moving bracelet is filtered by the least square method, the high-frequency noise is filtered by the low-pass filter, and the pressure data of the sensor is normalised by the *Z*-score method to realise the standardised processing of the moving Bracelet signal; According to the pre-processing results, the rigid structure model of human hand bone is constructed to reconstruct the posture of human hand. The RSSI signal is obtained by human-computer interaction technology, and the fingertip positioning and tracking of intelligent moving bracelet is realised by improving Kalman Filter algorithm. The following conclusions are drawn through experiments:

1) The fingertip positioning and tracking accuracy of the intelligent moving Bracelet based on this method is up to 97.9%. This shows that the proposed method has good tracking accuracy.

2) The fingertip positioning and tracking accuracy of the moving Bracelet proposed in this paper can reach 97.6%. This shows that this method can improve the positioning and tracking effect of Bracelet fingertips.

References

Chen, G., Chen, W. and Yu, H. (2019) 'Research on target tracking method of monocular vision underwater vehicle based on deep learning', *Machine Tools and Hydraulics*, Vol. 47, No. 23, pp.79–82.

Chen, L. (2020) 'Research on optimal location method of human motion target points based on image tracking', *Journal of Zhoukou Normal University*, Vol. 37, No. 2, pp.125–128.

Chen, L. and Li, J. (2020) 'Target tracking simulation of subsequent frame video image based on Visual Communication', *Computer Simulation*, Vol. 37, No. 4, pp.347–351.

Duan, C., Wang, J. and Deng, Z. (2020) 'Pseudo satellite dynamic tracking and positioning algorithm based on square root UKF', *Journal of Hebei University of Science and Technology*, Vol. 41, No. 6, pp.493–499.

Liu, K. and Gong, D. (2019) 'Multi target distribution estimation algorithm for fingertip location', *Journal of Zhengzhou University (Engineering Edition)*, Vol. 40, No. 4, pp.68–72+79.

Liu, Z., Zhu, S., Zhai, J. and Zhang, H. (2020) 'Video foreground motion tracking and region of interest capture', *Journal of Huazhong University of Science and Technology (Natural Science Edition)*, Vol. 48, No. 6, pp.1–5 + 12.

Ma, G. and Liu, L., Yu, Z., Cao, G. and Wang, Q. (2019) 'Calibration method of 3D topography measurement system based on IGPS positioning and tracking', *China Laser*, Vol. 46, No. 1, pp.179–187.

Tian, M., Ma, M. and Zhang, W. (2019) 'Target location and tracking based on azimuth measurement and velocity estimation', *Journal of Terahertz Science and Electronic Information*, Vol. 17, No. 1, pp.69–73.

Wu, J. and Feng, F. (2019) 'Research on warehouse location and tracking system based on multi-sensor information fusion', *Computer Technology and Development*, Vol. 29, No. 6, pp.134–137.

Xiu, C., Li, X. and Ba, F. (2019) 'Moving target tracking based on fuzzy histogram model', *Journal of Intelligent Systems*, Vol. 14, No. 5, pp.939–946.

Xu, G., An, Y., Yang, F., Zhang, Q. and Jin, S. (2020) 'Passive location and tracking of short-range moving small targets based on combined linear array', *Applied Acoustics*, Vol. 39, No. 1, pp.149–156.

Xu, X. and Hu, Y. (2019) 'A new method for location and tracking of responders in buildings', *Journal of Electronic Measurement and Instrument*, Vol. 33, No. 4, pp.111–118.

Yao, L., Pitla, S.K., Yang, Z., Xia, P., Zhao, C. (2019) 'Research on path tracking of mobile platform in agricultural facilities based on UWB wireless positioning', *Journal of Agricultural Engineering*, Vol. 35, No. 2, pp.17–24.

Zhang, J. and Hu, Z. (2020) 'Automatic moving target tracking method of intelligent monitoring system based on binocular vision', *Manufacturing Automation*, Vol. 42, No. 5, pp.142–146.

Zhang, X., Xu, Y., Qin, B. and Liu, Z. (2021) 'Harmonic source location method based on orthogonal matching tracking algorithm', *Electrical Measurement and Instrumentation*, Vol. 58, No. 4, pp.44–51.

Zheng, X., Xu, F. and Yang, J. (2020) 'Simulation of an improved underwater small target tracking algorithm', *Computer Simulation*, Vol. 37, No. 1, pp.244–248 + 443.